

THE FLUORAPATITES IN VOLCANIC PRODUCTS OF SOMMA-VESUVIUS VOLCANIC COMPLEX: CRYSTALLOGRAPHIC PARAMETERS, CRYSTAL-CHEMISTRY AND MINEROGENETIC IMPLICATIONS

MANUELA ROSSI

Dipartimento di Scienze della Terra, Università "Federico II", Via Mezzocannone 8, 80134 Napoli

INTRODUCTION

New mineralogical and geochemical data of ejecta from Somma-Vesuvius volcanic complex are reported here. There are various studies on these ejecta and mainly concern cumulitic and magmatic intrusive samples and recrystallized carbonate rocks from sedimentary basement. (Belkin *et al.*, 1985; De Vivo *et al.*, 1993; Cioni *et al.*, 1999; Gilg *et al.*, 2001; De Vivo *et al.*, 2001; Paone, 2006; Lima *et al.*, 2007). The ejecta examined in this work have very different compositions and most of the samples, coming from the Collection Vesuviana of Naples Royal Mineralogic Museum (Italy) and belonging to 1631 and 1872 eruptions, are more or less altered volcanic rocks.

On the basis of composition, structural and textural feature the samples have been divided in the following four types:

a) the samples 529b, 1535, 5895, 5896 are formed by two different and more or less vesiculated lavas (leucititic tephrites and leucititic tephrite-phonolites) separate from a micro-crystalline aggregate of fluorapatite, clinopyroxene, cancrinite, oxides and rare plagioclase (Fig. 1);

b) the samples 5644, 1528, 5886 and 5887 are formed by one lava (1528, 5886, 5887) or two lavas (5644) with compositions ranging from leucititic tephrites to leucititic tephrite-phonolites;

c) the samples 11299 and 11300 are formed by very altered lavas (leucititic tephrites) mantled by late minerals such as fluorapatite, sellaite, gypsum, wagnerite and phlogopite;

d) the samples 1601, 1602, 1785, 7377 and 5969 are formed by a leucititic tephritic lava and macro-crystalline aggregates of clinopyroxene, phlogopite and fluorapatite.

This work is mainly focused on the analysis of relationships between crystallographic parameters and crystal-chemistry of fluorapatite grains showing different textural features.

The aim of this paper is to give information on chemical and physical condition of magmatic chamber and sometimes, when is possible, to give information also on the interaction between the magma and fluids and/or brines.

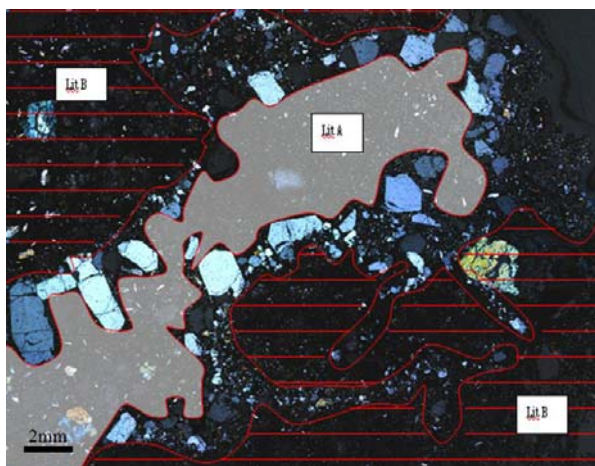


Fig. 1 - Photomicrographs with cross polarized light (XPL). Fluorapatites type 1 in contact with leucititic tephrites (Lit B) and leucititic tephrite-phonolites (Lit A), is associated with clinopyroxene, cancrinite group minerals, oxides and rare plagioclase (sample 1535).

ANALYTICAL TECHNIQUES

Major and minor elements were obtained with WDS (Cameca SX50) at CNR-IGAG of Rome, trace elements in minerals with laser-ablation microprobe linked with an inductively coupled plasma mass spectrometer (LAM-ICP-MS) at the CNR Istituto di Geoscienze e Georisorse, Pavia (Italy), analysis FT-IR on crystals of fluorapatite, with Jasco FT/IR 3000, INNOVA-CNR of Pozzuoli.

Morphological analyses were obtained with SEM-EDS (Jeol JSM 5310), at Centro Interdipartimentale di Strumentazioni per Analisi Geomineralogiche (CISAG), University of Naples “Federico II” (CISAG).

Modal analyses were obtained with axiovision rel. 4.8, modules Panorama and Automeasure.

The crystal chemical features of fluorapatite samples, have been examined by means of powder - (WaxS X-Pert Pro, Panalytical diffractometer, ICTP-CNR-INNOVA, Pozzuoli) and single crystal - X-ray diffractometry (Nonius Kappa CCD diffractometer, IC-CNR, Bari). Structural resolution was obtained with SIR97 (Altomare *et al.*, 1999) and SHELX97 (Sheldrick, 1997).

Fluid-inclusion studies were carried out on doubly polished wafers of about 500 μm thickness using a Linkam THM 600 at Dipartimento di Geofisica e Vulcanologia, University of Naples “Federico II”. The stage was calibrated at -56.6 , -6.6 , 0 , 51.1 , 93.8 , 163.8 and 398°C using both salts of known melting points and synthetic fluid inclusions. Calibration indicates a precision at the standard reference points of $\pm 0.7^\circ\text{C}$ at 0°C ; in the heating mode, calibration gives a precision of $\pm 6^\circ\text{C}$ at 398°C . High temperature measurements were carried out on a Linkam TH 1500 heating stage calibrated using different synthetic chemicals (KI: 681°C , BaCl_2 : 963°C , Au: 1063°C). The precision at 1063°C is $\pm 15^\circ\text{C}$.

OCCURRENCE, PARAGENESIS AND DISCUSSION

In the ejecta were recognized 5 fluorapatites types characterized by different crystallographic parameters and chemical composition.

The fluorapatites type 1 (samples 529b, 1535, 5895, 5896), in contact with leucititic tephrites and leucititic tephrite-phonolites rocks, are associated with clinopyroxene, cancrinite group minerals, oxides and rare plagioclase. These fluorapatites have euhedral form, prismatic hexagonal habit, are transparent, colourless and fluorescent at low and high wavelength. From a geochemical point of view, the fluorapatites type 1 have (Table 2 and 3) S, Si, As and V, which replaces P (Fig. 2), in tetrahedral site; Mn, Na_2O and higher REE in the cationic site; F, Cl and OH in the anionic site. Therefore, on the basis of chemical data, the possible substitutions in the different sites include: $(\text{VO}_4)^{3-} = (\text{PO}_4)^{3-}$, $(\text{AsO}_4)^{3-} = (\text{PO}_4)^{3-}$, $(\text{SO}_4)^{2-} + (\text{SiO}_4)^{4-} = 2 (\text{PO}_4)^{3-}$, $(\text{SO}_4)^{2-} + \text{Na}^+ = 2 (\text{PO}_4)^{3-} + \text{Ca}^{2+}$, $\text{REE}^{3+} + (\text{SiO}_4)^{4-} = \text{Ca}^{2+} + (\text{PO}_4)^{3-}$, $\text{REE}^{3+} + \text{Cl}^- = \text{Ca}^{2+} + \text{F}^-$, $\text{REE}^{3+} + \text{Na}^+ = 2 \text{Ca}^{2+}$, $\text{REE}^{3+} + \square = 3 \text{Ca}^{2+}$, $\text{Mn}^{2+} = \text{Ca}^{2+}$, $\text{OH}^- = \text{F}^-$ (Fleet *et al.*, 1997; Pan *et al.*, 2002; Parat *et al.*, 2004; Peng *et al.*, 1997; Piccoli *et al.*, 2002).

Single crystal X-ray analysis showed the isostructurality between the analyzed samples, solved within the hexagonal space group $P6_3/m$ (Table 1).

The crystallographic parameters were compared with fluorapatite, hydroxylapatite and clorapatite reported in Hughes *et al.* (1989, 2002).

The deviations of lattice parameters a and c may be due to the isomorphous substitutions in cationic and anionic sites. Changes induced in the natural apatites as a result of differences in the column anion propagate throughout the crystal structure. The effects on the Ca(1)O, polyhedral and the PO_4 tetrahedra are minor, whereas those on the Ca(2) $\text{O}_5\text{X(O)}$ polyhedron are significant (Hughes *et al.*, 1989).

The abundant presence of OH and LREE ($\text{La}_2\text{O}_3 = 0.239$ wt.%, $\text{Ce}_2\text{O}_3 = 1.122$ wt.%, and $\text{Pr}_2\text{O}_3 = 0.092$ wt.%) may be due to the structural deformation.

Table 1 - Crystal data, experimental condition and details of the single-crystal X-ray data collection (RT, MoK α , $\lambda = 0.71073$ Å) and structure refinement of Apatite fluorapatites type 1 and type 5.

	529b	1535
a (Å)	9.4280(5)	9.4300(8)
c (Å)	6.8810(2)	6.8760(4)
V (Å ³)	529.69(5)	529.53(7)
Calc. density (Mg·m ⁻³)	3.162	3.163
Absorption coeff. (mm ⁻¹)	3.067	3.067
$F(000)$	500	500
Crystal size (mm)	0.40 x 0.17 x 0.17	0.50 x 0.50 x 0.50
θ range for data collection	5.24° - 27.52°	5.24° - 27.51°
Limiting indices	-12 $\leq h \leq$ 12, -12 $\leq k \leq$ 11, -8 $\leq l \leq$ 8	-12 $\leq h \leq$ 12, -12 $\leq k \leq$ 12, -8 $\leq l \leq$ 8
Refl. collected / unique	6427 / 432 [$R(\text{int}) = 0.0260$]	5170 / 436 [$R(\text{int}) = 0.0518$]
Completeness to θ	97.5 %	98.4 %
Max. and min. transmission	0.6237 and 0.3734	0.3092 and 0.3092
Refinement method	FMLS	FMLS
Data / restraints / parameters	432 / 0 / 40	436 / 0 / 40
GOOF	1.136	1.176
Final R indices [$I > 2\sigma(I)$]	$R1 = 0.0153$, $wR2 = 0.0351$	$R1 = 0.0281$, $wR2 = 0.0759$
R indices (all data)	$R1 = 0.0153$, $wR2 = 0.0351$	$R1 = 0.0292$, $wR2 = 0.0766$
Extinction coefficient	0.057(3)	0.061(7)
Larg. diff. peak and hole (e Å ⁻³)	0.294 and -0.322	0.591 and -0.714

Table 1 - (continued).

	1601	5969
a (Å)	9.3860(6)	9.4040(10)
c (Å)	6.8850(6)	6.8840(5)
V (Å ³)	525.29(7)	527.23(12)
Calc. density (Mg·m ⁻³)	3.188	3.177
Absorption coeff. (mm ⁻¹)	3.092	3.081
$F(000)$	500	500
Crystal size (mm)	0.35 x 0.12 x 0.12	0.50 x 0.30 x 0.30
θ range for data collection	5.02° - 27.47°	5.01° - 27.69°
Limiting indices	-11 $\leq h \leq$ 12, -12 $\leq k \leq$ 12, -8 $\leq l \leq$ 8	-12 $\leq h \leq$ 12, -12 $\leq k \leq$ 12, -8 $\leq l \leq$ 8
Refl. collected / unique	5468 / 432 [$R(\text{int}) = 0.0510$]	6251 / 431 [$R(\text{int}) = 0.0280$]
Completeness to θ	98.6 %	96.0 %
Max. and min. transmission	0.7079 and 0.4108	0.4584 and 0.3080
Refinement method	FMLS	FMLS
Data / restraints / parameters	432 / 0 / 40	431 / 0 / 40
GOOF	1.155	1.336
Final R indices [$I > 2\sigma(I)$]	$R1 = 0.0199$, $wR2 = 0.0476$	$R1 = 0.0181$, $wR2 = 0.0498$
R indices (all data)	$R1 = 0.0202$, $wR2 = 0.0479$	$R1 = 0.0314$, $wR2 = 0.0586$
Extinction coefficient	0.050(3)	0.052(5)
Larg. diff. peak and hole (e Å ⁻³)	0.451 and -0.500	1.030 and -1.641

Primary, secondary and perhaps pseudosecondary inclusions occur in the fluorapatite crystals. In this work only primary silicate-melt inclusions, representing the trapping of silicate melt that was presumably in (local) equilibrium with the host crystal, were studied. Primary inclusions consist of silicate glass and minor amount of small mineral phases randomly distributed; in addition, only one shrinkage bubble occurs. As concern the crystalline component, two different mineral-types are present; at present, is very difficult to define if they are precipitated from the melt after entrapment (they are daughter crystals) or are accidentally trapped. Hundred primary silicate-melt inclusions were homogenized and show an average temperature homogenization (Th) of $1054 \pm 10^\circ\text{C}$.

The clinopyroxene, texturally coeval to fluorapatite grains, are crystallized to near 3 kbar.

The fluorapatites type 2 (samples 11299, 11300), cover very altered leucititic tephrites rocks, and are associated with sellaite, wagnerite, phlogopite and gypsum (Fig. 3). Often, these fluorapatites found in vesicles of altered lava, they have euhedral form and prismatic hexagonal habit, they are transparent and yellow. The geochemical analyses (Table 2 and 3) show higher amounts of S and lower Si (Fig. 2), As and V, which replaces P, in tetrahedral site; lower Fe, Mn, Mg, Sr, K and REE and Na replaced Ca in cationic site; F, Cl and lower OH occur in anionic site. Therefore, on the basis of chemical data, the possible substitutions in the different sites include: $(\text{SO}_4)^{2-} + \text{Na}^+ = 2 (\text{PO}_4)^{3-} + \text{Ca}^{2+}$, $\text{REE}^{3+} + (\text{SiO}_4)^{4-} = \text{Ca}^{2+} + (\text{PO}_4)^{3-}$, $\text{REE}^{3+} + \text{Cl}^{2-} = \text{Ca}^{2+} + \text{F}^-$, $\text{REE}^{3+} + \text{Na}^+ = 2 \text{Ca}^{2+}$, $\text{OH}^- = \text{F}^-$ (Fleet *et al.*, 1997; Pan *et al.*, 2002; Parat *et al.*, 2004; Peng *et al.*, 1997; Piccoli *et al.*, 2002).

In the fluorapatite type 2 crystals are presents secondary and sometimes primary melt inclusions. Were studied only primary melt inclusions. They consist now in silicate glass, various daughter mineral(s) plus a shrinkage bubble, or in glass plus a shrinkage bubble, sometimes in solid inclusions of phlogopite and oxides crystals. The inclusions studied, consist of silicate glass, one or more crystals (these have precipitated

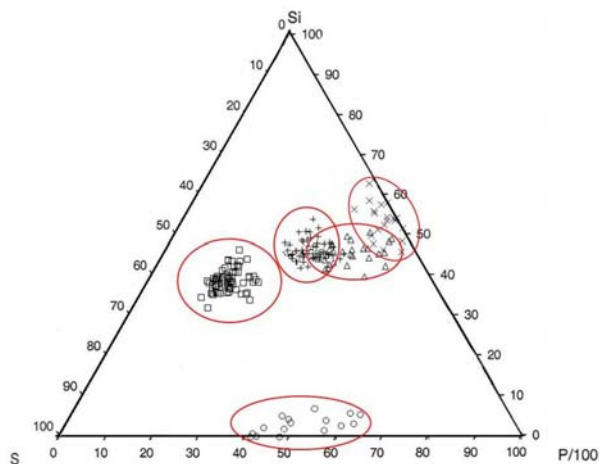


Fig. 2 - Plot of P/100, Si and S variability in fluorapatites types of ejecta from Somma-Vesuvius volcanic complex, belonging to 1631 and 1872 eruptions, calculated on apfu value (Piccoli & Candela, 2002).

□ = fluorapatites type 1; O = fluorapatites type 2; Δ = fluorapatites type 3; X = fluorapatites type 4; + = fluorapatites type 5.

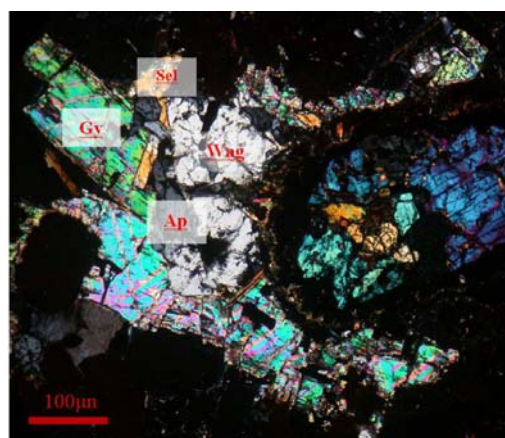


Fig. 3 - Photomicrographs with cross polarized light. fluorapatites type 2 (Ap) in vesicles with gypsum (Gy), sellaite (Sel) and wagnerite (Wag) (sample 11299).

with the mechanism similar to those reported for fluorapatites type 1) and shrinkage bubble. Twenty primary silicate-melt inclusions were homogenized, and show an average Th of $930 \pm 15^\circ\text{C}$.

Table 2 - Major and minor elements average composition (wt%) of apatites-(Ca-F) types.

Tipo	Type 1		Type 2		Type 3		Type 4		Type 5	
n.o.a	(61)	σ	(16)	σ	(47)	σ	(18)	σ	(91)	σ
SiO₂	0.754	0.114	0.020	0.015	0.424	0.064	0.441	0.074	0.488	0.098
Al₂O₃	0.006	0.007	0.007	0.008	0.007	0.009	0.011	0.011	0.006	0.008
FeO	0.039	0.030	0.113	0.057	0.249	0.134	0.210	0.068	0.194	0.088
MnO	0.131	0.041	0.048	0.050	0.054	0.037	0.055	0.021	0.042	0.029
MgO	0.363	0.027	0.371	0.142	0.261	0.070	0.267	0.041	0.231	0.028
CaO	54.041	0.778	55.195	0.660	54.861	0.865	54.737	0.588	54.975	0.955
SrO	0.130	0.046	0.070	0.034	0.256	0.042	0.260	0.059	0.266	0.058
Na₂O	0.280	0.051	0.161	0.043	0.049	0.027	0.067	0.033	0.053	0.020
K₂O	0.016	0.013	0.011	0.011	0.016	0.018	0.015	0.016	0.013	0.012
P₂O₅	38.555	0.732	41.505	0.488	40.348	0.823	41.039	0.541	39.978	0.970
SO₃	1.132	0.260	0.443	0.142	0.210	0.100	0.034	0.030	0.332	0.082
V₂O₅	0.313	0.054	0.013	0.017	0.025	0.030	0.024	0.031	0.035	0.079
As₂O₅	0.091	0.040	0.079	0.069	0.000	0.002	0.001	0.005	0.001	0.003
F	3.293	0.099	3.552	0.118	3.544	0.130	3.479	0.135	3.576	0.181
Cl	0.371	0.075	0.301	0.079	0.550	0.123	0.408	0.055	0.636	0.106
Tot.	99.508		101.888	0.000	100.854	0.000	101.047	0.000	100.825	0.000
(F,Cl)/O	1.469		1.563	0.000	1.616	0.000	1.557	0.000	1.649	0.000
Tot.	98.039		100.324		99.238		99.491		99.176	
Chemical formulae based on 16 cations										
Si	0.129		0.007		0.072		0.075		0.084	
Al	0.001		0.001		0.001		0.002		0.001	
Fe²⁺	0.005		0.016		0.035		0.030		0.028	
Mn	0.019		0.007		0.008		0.008		0.006	
Mg	0.093		0.093		0.066		0.067		0.059	
Ca	9.866		9.866		9.940		9.881		9.974	
Sr	0.013		0.007		0.025		0.026		0.026	
Na	0.093		0.052		0.016		0.022		0.017	
K	0.004		0.002		0.004		0.003		0.003	
P	5.587		5.888		5.803		5.880		5.756	
S	0.145		0.056		0.027		0.004		0.042	
V	0.035		0.002		0.003		0.003		0.004	
As	0.009		0.008		0.000		0.000		0.000	
F	1.783		1.882		1.904		1.862		1.924	
Cl	0.106		0.086		0.158		0.117		0.183	
OH	0.115		0.032		-0.062		0.021		-0.107	

The estimate standard deviations (σ) are indicated only for oxides on the basis of point analyses (n.o.a)

Table 3 - Trace elements average composition (ppm) of apatites-(Ca-F) types.

REEs	Type 1	Type 2	Type 3	Type 4	Type 5
n.o.a	(29)	(13)	(29)	(14)	(43)
Cs	0.02	0.14	0.10	0.23	0.05
Rb	0.15	1.58	1.68	2.17	0.63
Ba	39.47	10.20	161.13	124.38	89.02
Th	232.32	24.20	25.53	348.91	22.77
U	5.96	0.14	10.80	29.50	9.20
Nb	0.29	5.32	0.80	3.56	0.08
Ta	0.02	0.48	0.06	0.07	0.01
La	1035.33	264.70	384.61	1480.93	367.64
Ce	4750.86	1038.22	1428.80	4571.87	1412.88
Pb	13.53	7.53	19.73	26.10	21.13
Pr	396.31	142.56	132.44	458.60	125.72
Nd	1301.98	643.43	449.18	1465.68	433.31
Hf	0.09	4.57	0.14	1.27	0.14
Zr	11.08	109.92	6.08	35.76	4.87
Sm	235.43	166.70	80.61	267.72	76.49
Eu	60.58	47.45	21.94	49.20	20.25
Gd	149.74	146.12	54.04	189.14	52.09
Ti	5.19	11622.40	77.85	131.81	36.11
Tb	18.46	19.30	5.84	24.02	5.90
Dy	89.84	97.10	26.87	109.30	26.51
Y	436.19	379.48	112.60	541.55	113.18
Ho	15.76	18.20	4.22	19.28	4.40
Er	37.19	41.85	8.80	44.44	9.04
Tm	4.78	5.17	1.03	5.79	1.07
Yb	30.29	30.37	5.60	33.81	5.75
Lu	4.00	3.95	0.75	4.80	0.72

n.o.a = point analyses

The fluorapatite type 3 (samples 529b, 1535, 5895, 5644, 11299, 1528, 5887, 1602, 1785, 1602, 5969, 7377, 11299, 11300), occurs in the phenocrystals of clinopyroxene (Fig. 4) and rarely olivine, as microlites and in glomeroporphyric aggregates all embodied in leucititic tephrites and leucititic tephrite-phonolites. The crystals have subeuhedral form and elongated habit. From a geochemical point of view these apatite have lower S (very low for apatites in aggregates glomeroporphyric;) and higher Si in substitution of P (Fig. 2); they have REE and Fe in substitution of Ca. In anionic site are present mainly F and Cl. For the apatite type 3 the possible substitutions include: $\text{REE}^{3+} + \text{Cl}^{2-} = \text{Ca}^{2+} + \text{F}^-$, $(\text{SO}_4)^{2-} + (\text{SiO}_4)^{4-} = 2 (\text{PO}_4)^{3-}$ and $\text{REE}^{3+} + (\text{SiO}_4)^{4-} = \text{Ca}^{2+} + (\text{PO}_4)^{3-}$ (Fleet *et al.*, 1997; Pan *et al.*, 2002; Parat *et al.*, 2004; Peng *et al.*, 1997; Piccoli *et al.*, 2002).

The fluorapatites type 4 (5644, 1528, 5886 and 5887) are in vesicles of leucititic tephrite-phonolites, they are associated with phlogopite, magnetite, clinopyroxene and orthoclase (Fig. 5); they have euhedral

form, prismatic hexagonal humpty dumpty habit and white-yellow colour. From a geochemical point of view the apatite type 4 presents in substitution of P, Si and lower S (Fig. 2); in substitution of Ca in cationic site, higher REE (Fig. 6), and lower Fe, Na and Mn; F, Cl and lower OH in anionic site. The possible substitutions include: $REE^{3+} + (SiO_4)^{4-} = Ca^{2+} + (PO_4)^{3-}$, $REE^{3+} + Na^+ = 2 Ca^{2+}$, $REE^{3+} + Cl^{2-} = Ca^{2+} + F^-$, $OH^- = F^-$ (Fleet *et al.*, 1997; Pan *et al.*, 2002; Parat *et al.*, 2004; Peng *et al.*, 1997; Piccoli *et al.*, 2002).

In the apatite type 4 crystals, secondary and rarely primary melt inclusions are presents. Were investigated only primary melt inclusions that consist of silicate glass, plus a shrinkage bubble. Twenty primary silicate-melt inclusions were homogenized, and show an average Th of $955 \pm 20^\circ C$.

The fluorapatites type 5 (1601, 1602, 1785, 5969, 7377) are with clinopyroxene and phlogopite in macro-crystalline aggregates. These crystals of apatite have euhedral form, prismatic hexagonal elongated habit and yellow colour. They are characterized by presence of elongated central vugs and inclusions melt and fluid inclusions) parallel with axis *c* (Fig. 7). The chemical composition and the principal substitutions in anionic and cationic sites are very similar at fluorapatites type 3 (Fig. 2 and 5).

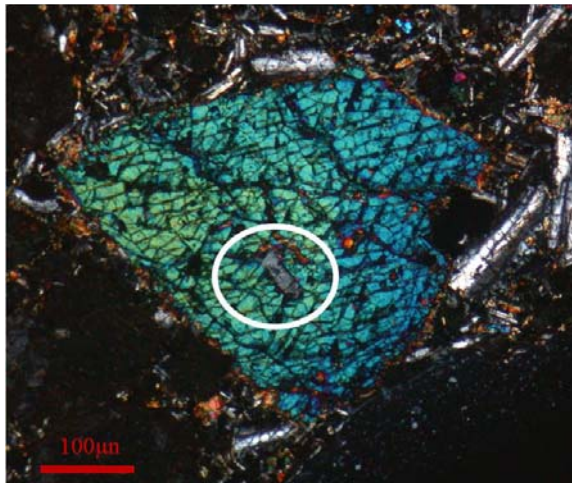


Fig. 4 - Photomicrographs with cross polarized light. fluorapatites type 3 in the phenocrysts of clinopyroxene (sample 1528).

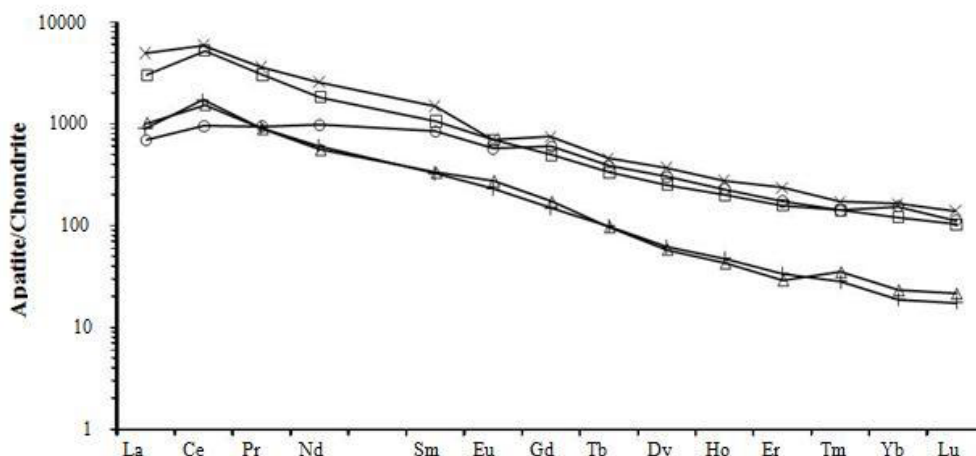


Fig. 5 - Chondrite-normalized average REE patterns for fluorapatites types of ejecta from Somma-Vesuvius volcanic complex, belonging to 1631 and 1872 eruptions.
 □ = fluorapatites type 1; ○ = fluorapatites type 2; Δ = fluorapatites type 3; × = fluorapatites type 4; + = fluorapatites type 5.



Fig. 6 - Micrograph . Fluorapatites type 4(Ap) in vesicles, with phlogopite (phl), orthoclase (Or) and oxides (sample 5644).



Fig. 7 - Photomicrographs with cross polarized light. Fluorapatites type 5 (ap) with clinopyroxene (cpx) and phlogopite (phl) in macro-crystalline aggregates (sample 1601). The apatite crystal shows elongated central vugs and inclusions (melt and fluid inclusions) parallel with axis *c*.

Single crystal X-ray analyses are made on these fluorapatites, solved within the hexagonal space group $P6_3/m$ (Table 1).

The crystallographic parameters compared with those reported by fluorapatite, hydroxylapatite and chlorapatite in Hughes et al. (1989, 2002), do not show the particular differences. The chemical analysis confirms the limited substitution in Ca2 sites ($\text{La}_2\text{O}_3 = 0.077 \text{ wt.}\%$, $\text{Ce}_2\text{O}_3 = 0.378 \text{ wt.}\%$, and $\text{Pr}_2\text{O}_3 = 0.029 \text{ wt.}\%$) and the absence of OH in halogens site.

In fluorapatite type 5 crystals are presents abundant primary fluid and melt inclusions. Primary CO_2 inclusions in fluorapatite have usually a tubular shape, they are arrayed parallel to the *c*-axis of the host and they are in the cores of the grains. Hundred inclusions at CO_2 were studied: the T_h , determined in vapour phase, it changes from 29.5 to 30.5°C (corresponding to 1100-1200 kbar), the triple point changes from 57.2 to 57.6°C. The melt inclusions are tubular and show the typical shape, elongated in the (0001) direction. They consist of silicate glass, trapped mineral phases and/or daughter crystals (phlogopite, clinopyroxene and oxides crystals), plus a shrinkage bubble which may be single or multiple. As concern the crystalline component, two different minerals-types occur; at present, is very difficult to define if they are precipitated from the melt after entrapment (they are daughter crystals) or are accidentally trapped. Fifty primary silicate-melt inclusions were homogenized and present an average T_h of $1100 \pm 20^\circ\text{C}$.

CONCLUSION

The investigated fluorapatite show considerable variability in their geochemical compositions and structural features; it strongly suggest that they are crystallized in different minerogenetic system.

The five fluorapatite types can be reported to two principal minerogenetic system:

A. the fluorapatites type 3 can be reported to early phases formed together with clinopyroxene phenocrysts during a crystal fractionation process of alkaline magma. In these fluorapatites the low

content of REE is likely due to low activity of SiO₂ in the crystallizing magmas whereas the low concentration of SO₃, Ce₂O₃, and Eu₂O₃ is linked to low O₂ fugacity of the system. The fluorapatites type 4, crystallize together with phlogopite, orthoclase and fluorite, show major amounts of REE with the exception of Eu and present lower concentration of OH. Therefore, it is likely due to a major evolution degree of parental magma.

B. The fluorapatites type 1, 2, 5 and associated minerals require particular and unusual parental melts. Interaction processes between magmas and fluids and/or brines, derived from sedimentary rocks of basement, can give rise at particular melts characterized by:

1) high content of P, Ca, S and F, ratio Cl/OH \cong 1, high value of fugacity O₂ and high concentration of REE. In this system crystallize fluorapatite type 1, clinopyroxene, and cancrinite group minerals (with T of 1044°C and P of 2.86 kbar).

2) high content of P, Ca, S, Mg, K and F, ratio Cl/OH > 1, lower value of fugacity O₂ and lower concentration of REE. In this system crystallize fluorapatite type 2, sellaite, phlogopite, and wagnerite (with T of 935°C).

3) high content of Ca, P, K, S and F, very high Cl/OH ratio, lower value of fugacity O₂ and lower concentration of REE. In this system crystallized clinopyroxene, phlogopite and fluorapatite type 5 (with T of 1100°C and P of 1.04 kbar).

REFERENCES

- Altomare, A., Burla, M.C., Camalli, M., Cascarano, G.L., Giacobozzo, C., Guagliardi, A., Moliterni, A.G.G., Polidori, G., Spagna, R. (1999): SIR97: a new tool for crystal determination and refinement. *J. Appl. Crystallogr.*, **32**, 115-119.
- Belkin, E.H., De Vivo, B., Roedder, E., Cortini, M. (1985): Fluid inclusion geobarometry from Mt. Somma-Vesuvius nodules. *Am. Mineral.*, **70**, 288-303.
- Cioni, R., Santacroce, R., Sbrana, A. (1999): Pyroclastic deposits as a guide reconstructing the multi-stage evolution of the Somma-Vesuvius caldera. *Bull. Volcanol.*, **60**, 207-222.
- De Vivo, B. & Rolandi, G. (2001): Special issue on Mount Somma-Vesuvius. *Mineral. Petrol.*, **73**, 121-143.
- De Vivo, B., Scandone, R., Trigila, R. (1993): Special issue on Mount Vesuvius. *J. Volcanol. Geotherm. Res.*, **58**, 367-376.
- Fleet, M.E. & Pan, Y. (1997): Site preference of rare earth elements in fluorapatite: binary (LREE+HREE)-substituted crystals. *Am. Mineral.*, **82**, 870-877.
- Gilg, H.A., Lima, A., Somma, R., Belkin, H.E., De Vivo, B., Ayuso, R.A. (2001): Isotope geochemistry and fluid inclusion study of skarns from Vesuvius. *Mineral. Petrol.*, **73**, 145-176.
- Hughes, J.M. & Rakovan, J. (2002): The crystal structure of apatite, Ca₅(PO₄)₃(F,OH,Cl). *Rev. Mineral. Geochem.*, **48**, 1-12.
- Hughes, J.M., Cameron, M., Crowley, K.D. (1989): Structural variations in natural F, OH, and Cl apatites. *Am. Mineral.*, **74**, 870-876.
- Lima, A., De Vivo, B., Fedele, L., Sintoni, F., Milia, A. (2007): Geochemical variations between the 79 AD and 1944 AD Somma-Vesuvius volcanic products: constraints on the evolution of the hydrothermal system based on fluid and melt inclusions. *Chem. Geol.*, **237**, 401-417.
- Pan, Y. & Fleet, M.E. (2002): Composition of the apatite-group minerals: substitution mechanism and controlling factors. *Rev. Mineral. Geochem.*, **48**, 13-49.
- Paone, A. (2006): The geochemical evolution of the Mt. Somma-Vesuvius volcano. *Mineral. Petrol.*, **87**, 53-80.
- Parat, F. & Holtz, F. (2004): Sulphur partitioning between apatite and melt and effect of sulphur on apatite solubility at oxidizing conditions. *Contrib. Mineral. Petrol.*, **147**, 201-212.
- Pasero, M., Kampf, A.R., Ferraris, C., Pekov, I.V., Rakovan, J., White, T.J. (2010): Nomenclature of the apatite supergroup minerals. *Eur. J. Mineral.*, **22**, 163-179.

- Peng, G., Luhr, J.F., McGee, J.J. (1997): Factors controlling sulfur concentrations in volcanic apatite. *Am. Mineral.*, **82**, 1210-1224.
- Piccoli, P.M. & Candela, P.A. (2002): Apatite in Igneous Systems. *Rev. Mineral. Geochem.*, **48**, 255-292.
- Powder Diffraction Files Database (2009): International Centre for Diffraction Data. 12 Campus Blvd., Newtown Square, PA 19073-3273 U.S.A.
- Sheldrick, G.M. (1997): SHELXS97 and SHELXL97. University of Gottingen, Germany.